Azimuth Null-Reduced Radiation Pattern, Ultralow Profile, Dual-Wideband and Low Passive Intermodulation Ceiling Mount Antenna for Long Term Evolution Application

KOK JIUNN NG[1], **(Member, IEEE), MOHAMMAD TARIQUL ISLAM**[2], **(Senior Member, IEEE),**
ADAM ALEVY[3], **(Member, IEEE), MOHD. FAIS MANSOR**[2], **(Member, IEEE),**
AND CHOON CHUNG SU[1]
[1]Laird Connectivity, Perai 12000, Malaysia
[2]Center of Advanced Electronic and Communication Engineering, Universiti Kebangsaan Malaysia (UKM), Bangi 43600, Malaysia
[3]Laird Connectivity, Manchester, NH 03103, USA

Corresponding author: Mohammad Tariqul Islam (tariqul@ukm.edu.my)

ABSTRACT An ultralow profile, dual-wideband and low passive intermodulation (PIM) in-building ceiling-mount antenna for long term evolution (LTE) distributed antenna system (DAS) application is presented. The proposed antenna was designed based on asymmetrical dipole concept having a ground plane with an inclined feeding edge to achieve wideband characteristic and reduced null radiation pattern in the azimuth plane when oriented horizontally. Various dipole and monopole design approaches are presented to give an insight into the typical elevation dipole-liked radiation pattern in the azimuth plane when oriented horizontally to achieve ultralow profile feature. The proposed antenna improves from a simple rectangular monopole to a newly innovated design with off-center feeding location and radiating elements by implementing new design features, e.g. having variation between edges of the radiator and ground plane, slots within monopole radiator and ground plane and inclination of the feeding edge of the ground plane. These additional features enable the proposed design to have a good compromise between the azimuth plane radiation pattern and impedance matching. A production-quality prototype was fabricated to ensure the best PIM performance is achievable. The performance of the prototype was measured. The antenna offers dual-wideband characteristic covering most of the LTE frequency ranges of 698-960MHz and 1350-3800MHz. The passive intermodulation levels that measured for both 700MHz and 1920MHz bands are better than -150 dBc at carrier input of 2×20 Watts.

INDEX TERMS Broadband antennas, dipole antennas, antenna radiation patterns.

I. INTRODUCTION

With the explosive growth of mobile communication systems in recent years, ultralow profile antennas for indoor distributed antenna system (DAS) have gained increased popularity due to high expectation of aesthetically pleasing profile when integrated into the ceiling design of the building. This has become a new class of requirement in which stable and highly omnidirectional radiation pattern with vertical polarization has been gradually superseded by

The associate editor coordinating the review of this manuscript and approving it for publication was Neng Wu Liu.

quasi-omnidirectional with horizontal polarization and aesthetically attractive characteristics.

Conventional wideband omnidirectional antenna developed for single-input-single-output (SISO) DAS system is mainly monopole, biconical or variations of them that may have a typical internal size of about 185mm (dia.) × 76mm (h) as shown in Fig. 1 to cover the typical frequency range of 698-960 MHz and 1710-2700 MHz. However, these type of antennas are large in size and have led into extensive study on lower profile design using shorted top hat mono-cone antenna [1], complicated three patches monopole fed with coaxial with a three shorted legs coupling patch [2],

IEEE *Access*

K. J. Ng *et al.*: Azimuth Null-Reduced Radiation Pattern, Ultralow Profile, Dual-Wideband and Low PIM Ceiling Mount Antenna
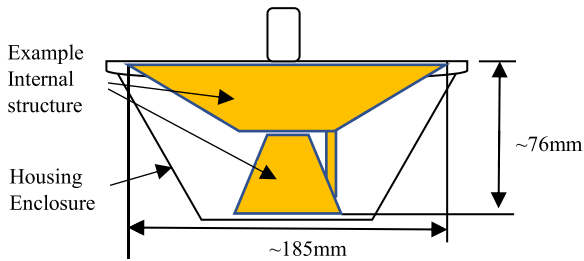

FIGURE 1. Side view of the conventional form factor of omnidirectional antenna for in-building DAS application.

combined spiral-discone antenna [3], complicated construction of truncated cone that loaded with three shorted coupling patches and a circular sleeve on the ground [4] and body of revolution (BOR) with a shorted parasitic ring (SPR) [5] that can achieve up to 148% bandwidth. However, the profile of all these antennas may not be low enough to have a thickness of about 7-10 mm to allow them looks flush to the ceiling.

For ultralow profile applications, design concept may have limited to printed slot and dipole antenna that oriented horizontally. Wideband, omnidirectional and horizontally-polarized designs have been reported such as circular array of eight tapered slots antenna [6], four wideband dipoles conducted as a loop antenna with parasitic strips [7], six tightly coupled dipole array [8], twelve printed and tightly coupled arc dipole array with rows of parasitic arc strips and directors [9] and four arc printed dipole array with four pairs of parasitic strips [10]. Although these antennas provide reasonably good omnidirectionality but have limited bandwidth. These antennas may be viable only for the high band (1.7-3.8 GHz) due to the acceptable size. To accommodate a dipole array of frequency as low as 698 MHz, the size of the antenna becomes too large. Therefore, a single element of wideband dipole antenna like a bow tie and circular or ellipse arms have become the candidates in considering the size factor of the antenna. However, these dipoles have deep nulls in its radiation pattern when oriented horizontally. The deep nulls have been a concern for the telecommunication operator due to the higher risk of unstable connectivity or blind spots at locations covered by the nulls. The reported works for other wideband or multiband single element antennas such as asymmetrical dipole of circular shape [11], elliptical monopole on trapezoid ground plane [12] and multiple folded radiating elements with multiband [13] are only focused on the bandwidth enhancement and its omnidirectionality for vertical polarization. There is not much attention was given on improving the deep nulls of the radiation pattern in the azimuth plane for ultralow profile antenna when it is horizontally polarized.

Other than the radiation pattern, low PIM antenna has become a necessary requirement to maximize throughput and capacity of a network in modern DAS system. Unfortunately, PIM levels are difficult to calculate, or measure and thus very little explicit documentation exists on the subject [14]. PIM generated from the non-linearities in the components'

power response and is a function of many variables. Unlike VSWR, PIM is not able to be gauged purely by the components' physical characteristics. Therefore, it may be difficult to identify the PIM source and involves more detailed and careful design considerations including material selection and preparation process, assembly process, workmanship and quality of the components of the assemblies.

In this work, we analyzed the characteristics of radiation patterns for several dipole and monopole antennas. The basic dipole that has reduced null in the azimuth plane was identified and further improved with added design freedom flexibility for more optimum performance of radiation pattern and impedance matching. The proposed design is based on asymmetrical dipole concept that has offset fed monopole radiating element with offset feed location on inclined edge ground plane. Although the proposed design is not able to provide pure omnidirectional radiation pattern, it offers reduced null in the radiation pattern of the azimuth plane compared to the deep null of the typical dipole that oriented horizontally. Due to the dipole antenna characteristic, this antenna is suitable for common plaster ceiling or ceiling tiles and not for the metal or aluminium panel and aluminium backed plaster ceiling tiles. In meeting consistent low PIM requirement, the antenna design proposed simple assembly approaches and suitable material selection. It may seem to be easy to achieve a low PIM printed antenna (PCB type) but it is difficult to maintain consistency and reproducibility of low PIM level in production. A prototype was fabricated and measured.

II. ANTENNA DESIGN AND ANALYSIS
A. SIMULATION ANALYSIS OF VARIOUS DIPOLE/MONOPOLE ANTENNA DESIGNS
Four antenna designs shown in Fig. 2 are based on dipole and monopole concepts. They are denoted as Type-I to Type-IV respectively. These antennas are used to give an insight into the characteristic of the various design approaches of dipole and monopole antennas. All the designs are optimized to cover wide LTE band that includes the frequency ranges of 698-960 MHz, 1350-1550 MHz and 1690-3800 MHz. Antenna Type-I is a conventional symmetrical bow-tie dipole antenna with additional steps of two slanted edges at its feeding point to provide extra flexibility for impedance matching. Antenna Type-II uses a non-symmetrical arm approach of
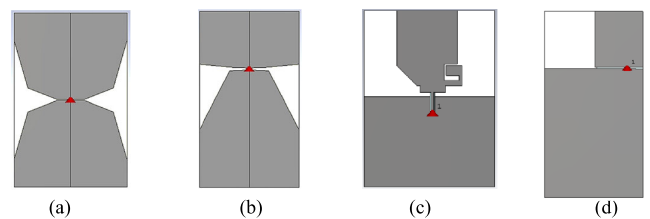

(a)   (b)   (c)   (d)

FIGURE 2. Dipole antenna configuration (a) Type-I (Symmetrical bow-tie), (b) Type-II (Asymmetrical bow-tie), (c) Type-III (Dual arm monopole) (d) Type-IV (Offset fed rectangle monopole).

K. J. Ng *et al.*: Azimuth Null-Reduced Radiation Pattern, Ultralow Profile, Dual-Wideband and Low PIM Ceiling Mount Antenna

IEEE *Access*

a bow-tie dipole antenna with a different slope of the edge between the top arm and bottom arms. Antenna Type-III is utilizing dual arms monopole radiating element fed from a flat edge ground plane. Antenna Type-IV is using a simple offset fed rectangular monopole and offsets feeding location at the ground plane. To investigate the radiation pattern characteristic, the structure of the antennas is simulated using the commercial simulation software CST microwave studio. The substrate used for these antennas is FR4 with a relative dielectric constant of 4.3 and tangent loss of 0.025.

All these antennas can be easily optimized to cover the full LTE band. Fig. 3 shows the VSWR of the dipole/monopole antennas. The bandwidth of Type-I and Type-II typically depending on the width and length of the arm as well as the gap and the slope of the edge of the arm at the feeding point. Antenna Type-III has split bands while antenna Type-I, Type-II and Type-IV offer a single wide frequency range of 698-3800MHz. Table 1 shows the dimension of these antennas. Antenna Type-III has the largest size of 130 mm × 176 mm and antenna Type-II has the smallest size.
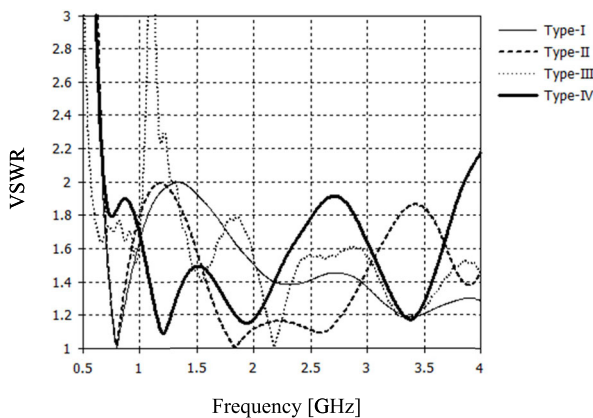

FIGURE 3. Simulated VSWR for antenna type-I, type-II, type-III and type IV.

TABLE 1. Antenna Type-I, Type-II, Type-III, Type-VI and proposed design description and size that have been optimized to cover LTE band.

Antenna type	Description	Width (mm)	Length (mm)
Type-I	Symmetrical Bow-Tie	95	147
Type-II	*Asymmetrical Bow-Tie*	79.42	145
Type-III	*Dual Arm Monopole*	130	*176*
Type-IV	*Offset Rectangle Monopole and offset feeding point*	94	180
Proposed Design	*Offset Monopole offset feeding point and slant feeding edge ground plane*	90	151

For the sake brevity, only the radiation pattern for azimuth plane is presented to avoid too many plots due to the wide bandwidth and irregular radiation patterns across the

frequency range. Fig. 4 shows the azimuth planes when the antennas are oriented horizontally. Antenna Type-I shows the typical dipole radiation pattern across the frequency of interest while antenna Type-II and Type-III more alike to
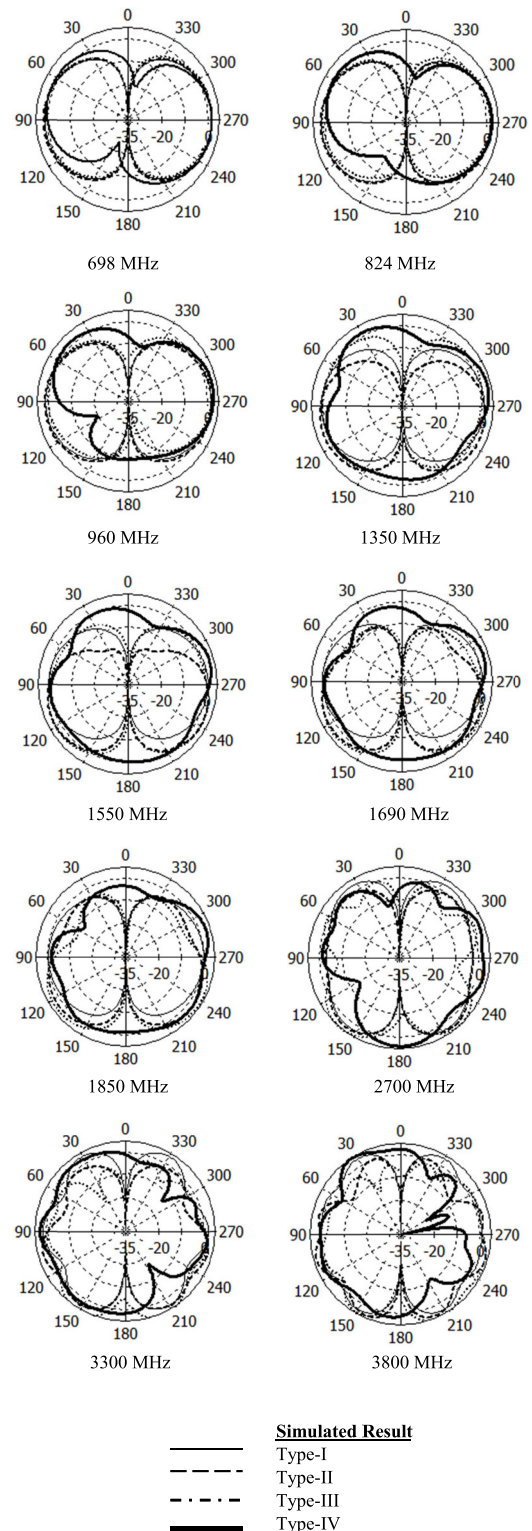

FIGURE 4. Comparison of the radiation pattern of the conventional symmetrical and asymmetrical dipole antenna at Azimuth Plane.

typical monopole radiation pattern, especially at the higher frequencies. Some may regard them as asymmetrical arm dipole where the longer arm may serve as bigger ground plane and have the additional mode. Antenna Type IV shows an interesting characteristic that has reduced null across most of the band except a very deep null at 3800 MHz. Antenna Type-IV has flat surface between the monopole edge and the ground plane edge at the feeding and it has offset monopole as well as offset feeding point. This contributes to the better radiation pattern characteristic and was part of the proposed design. Such a simple construction may have limited parameter to optimize for both good radiation pattern and VSWR simultaneously for the antenna. It is constraint by the gap between the monopole radiator and ground plane and the flat edge at the feed.

B. PROPOSED ANTENNA DESIGN GEOMETRY

Fig. 5 depicts the geometry of the printed antenna on a substrate. The substrate used is AD300 laminate with relative dielectric constant, $\varepsilon_r = 3$ and thickness of 0.76 mm. The substrate size is 151 mm × 90 mm. The antenna consists of a monopole radiating element at the top layer of the substrate. The monopole radiating element is fed at offset location like antenna Type-IV but different gap Gap_1 and Gap_2 are

introduced between the monopole radiating element and feeding edge of the ground plane. Slots S_{L2}, S_{W2}, S_{L3}, and S_{W3} are introduced into the monopole radiating element. The monopole has two-steps width R_{W1} and R_{W2}. The monopole radiator is fed with microstrip line M_{W1} and M_{L2} which can ease the impedance matching for the antenna. The monopole inclines in parallel to the feeding edge of the ground plane inclination angle, θ. The monopole radiating element is fed from the right edge as feed position F_p. Slots S_{W1}, S_{L1}, and S_{P1} are located at the inclined feeding edge of the ground. With the introduction of various tunable parameters, the antenna has more design freedoms in considering both VSWR and improving the null of the radiation pattern at the same time. The antenna transmission line is terminated with a 355.8mm length pigtail coaxial cable which translated into about 300mm pigtail cable length, C_Length from the plastic stud. This cable length is typical for industry ceiling mount product. Table 2 summarized the antenna parameters.

TABLE 2. Proposed antenna parameters.

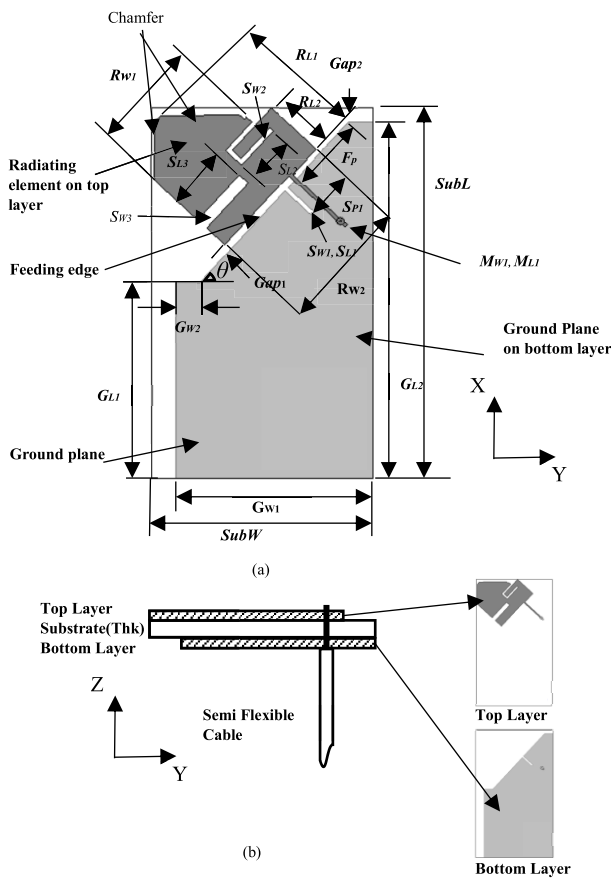| Parameters	Value(mm)	Parameters	Value (mm)
G_{W1}	80	R_{L1}	53.85
G_{W2}	10	R_{L2}	24.75
G_{L1}	80	R_{W1}	43.00
G_{L2}	145	R_{W2}	53.90
S_{W1}	1.77	Gap_1	3.10
S_{L1}	14.77	Gap_2	2.15
S_{W2}	2.00	FP_p	30.76
S_{L2}	19.00	Thk	0.76
S_{W3}	4.90	$SubW$	90
S_{L3}	24.90	$SubL$	151
M_{W1}	1.40	M_{L1}	26.66

FIGURE 5. The geometry of the proposed design with (a) superimposed of the top layer and bottom layer and (b) side view and the illustration of the layers of the copper trace.

The housing and assembly features of the antenna are specifically designed for practical applications. The design consists of a plastic top housing, a plastic base plate with stud and a printed circuit board (PCB) fed with a cable assembly as shown in Fig. 6. The dimension of the plastic housing is 180.3 mm x 117.2 mm × 7.6 mm. This thickness is ultralow profile compared to conventional standard antenna size of 185mm (dia.) × 86mm (H) as a finished product.

As the proposed antenna is an unbalanced dipole with pigtail cable, its performance will be affected slightly by the pigtail cable length. Therefore it is essential that the antenna is simulated with the exact length of the cable to have the result conform to the measurement result.
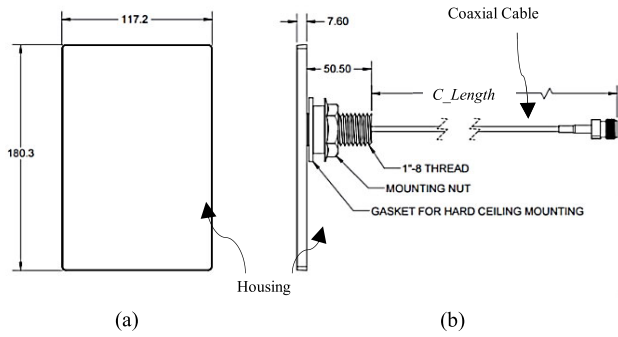
K. J. Ng *et al.*: Azimuth Null-Reduced Radiation Pattern, Ultralow Profile, Dual-Wideband and Low PIM Ceiling Mount Antenna

IEEE *Access*

FIGURE 6. The form factor of the proposed low-profile ceiling mount antenna with pigtail cable. (a) Top view and (b) side view.

C. EFFECT OF FEEDPOINT LOCATION AND INCLINATION ANGLE OF FEEDING EDGE OF GROUND PLANE

Like antenna type-IV, the feed point, F_p from right edge plays an important role to reduce the null level of the radiation pattern especially for the frequency range 1550-3800 MHz. Fig. 7 shows the parametric studies on the effect of feed point location, F_p. All other parameters were kept constant to the value shown in Table 2. We noted that the return loss degraded when F_p moved to the center and the optimum F_p is 31.5mm. Fig. 8 shows the effect on simulated azimuth plane radiation pattern when F_p moves to the center. The azimuth plane radiation pattern shows degradation with deeper nulls or reduced gain especially for the frequency range of 1350-1850 MHz.
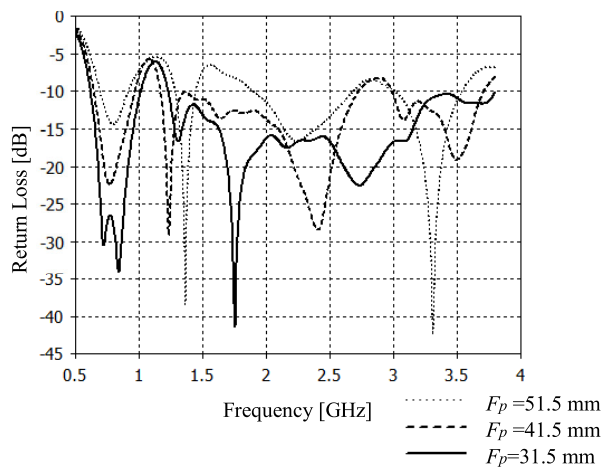
FIGURE 7. Parametric study of the feed point, F_p location from the right-hand corner ground edge on return loss.

As there are parameters that are interdependent, the impedance of the antenna can be matched with various combinations between them. The inclination angle, θ of the feeding edge of the ground plane is one of the important factors that affect the radiation pattern. To give a better insight into the effect, two inclination angles of $\theta = 4.3°$ and 47.3° with other parameters optimized to match to the same desired operating frequency range. The radiation pattern of the azimuth plane is presented in Fig. 9. We noted that the
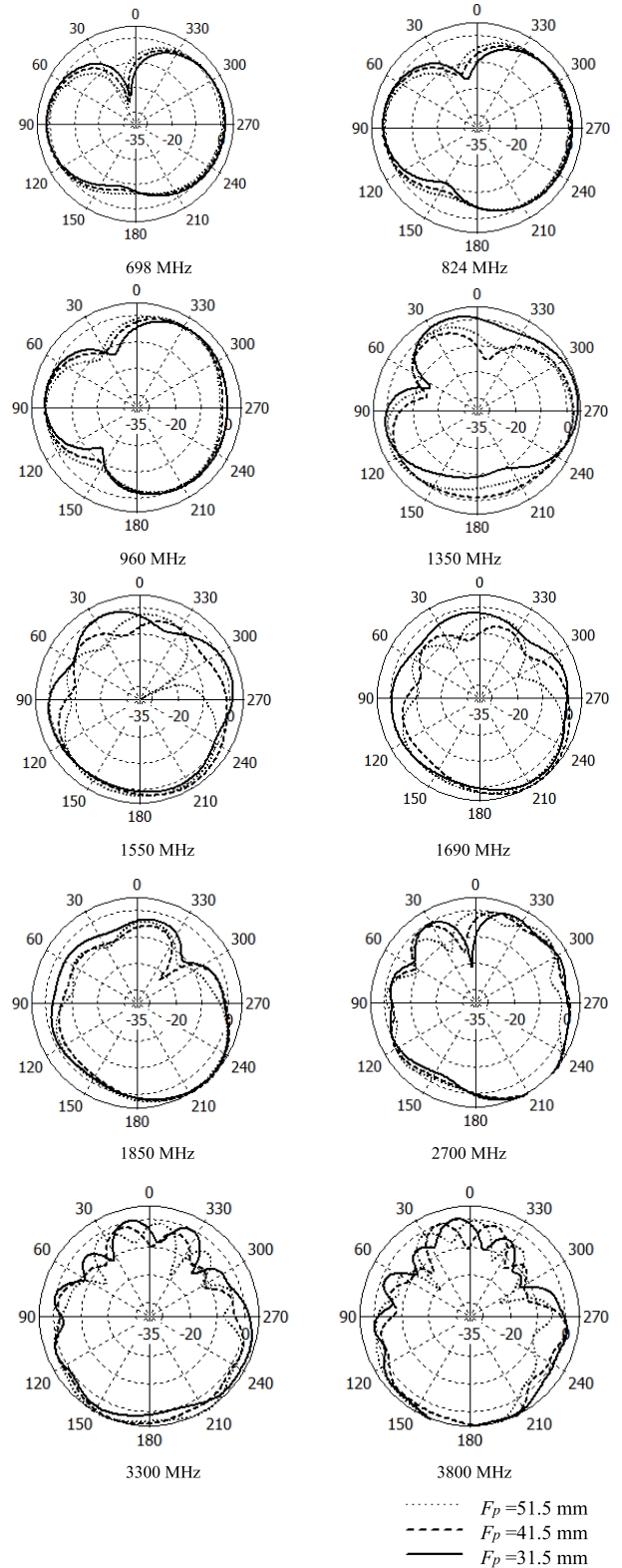

FIGURE 8. Radiation pattern effect by the F_p on the slanted edge ground plane.

inclination angle, $\theta = 4.3$ has deeper nulls or reduced gain compared to $\theta = 47.3$ for the frequency range of 1690 to 1850 MHz. To match the antenna with the inclination angle,

698 MHz

824 MHz

960 MHz

1350 MHz

1550 MHz

1690 MHz

1850 MHz

2700 MHz

3300 MHz

3800 MHz

- - - - - Inclination angle, θ=4.3°
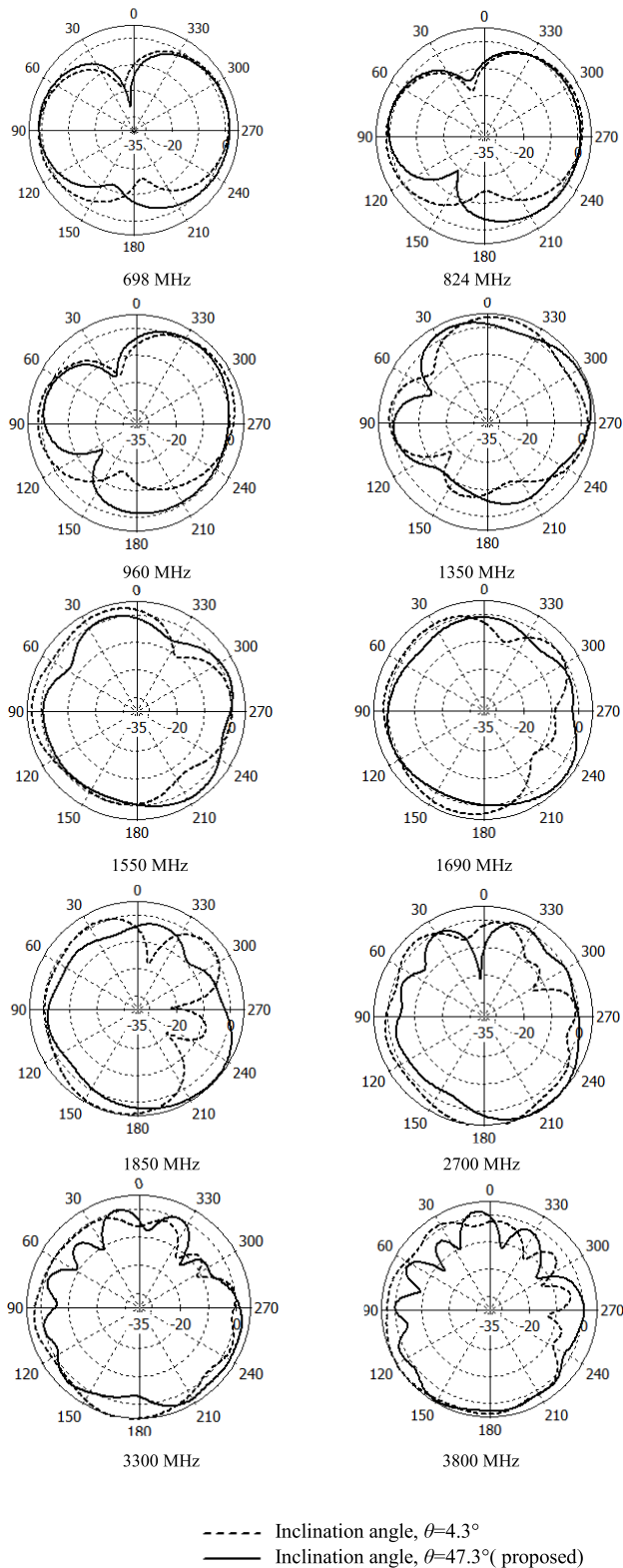——— Inclination angle, θ=47.3°(proposed)

FIGURE 9. Radiation pattern effect by the similar proposed radiating elements on low inclination angle ground edge plane with some parameters change (F_P = 41mm, S_{L3}=14mm, S_{L2} = 18 mm, $gap1$ = 1.5mm, G_{L1} = 100mm) to match the VSWR < 2:1 across the LTE Band.

$\theta = 4.3$, the feed point (F_p) was moved to the center that causes degradation of the radiation pattern in the mentioned frequency range. For inclination angle, $\theta = 47.3$ other

parameters S_{L3}, S_{L2}, Gap_1, and G_{L1} are optimized accordingly. The optimized antenna with inclination $\theta = 47.3$ demonstrated superior radiation pattern compared to antenna type IV for frequency range 2700-3800MHz.

D. EFFECT OF SLOTS AND GAPS

There are three slots introduced in the proposed antenna with one at the feeding edge of the ground plane and the other two at the monopole radiator. Fig. 10 and Fig. 11 show the parametric studies on the effect of slot length S_{L1} and position S_{LP} at the feed ground plane edge on the return loss and impedance locus, respectively. Other parameters are kept constant. The return loss for the low-frequency range of 698-960MHz improves when the S_{L1} increases to 10mm where the impedance locus becomes less resistive and move to the center of the Smith chart. However, a drastic degradation in return loss in the 3500 MHz band is observed when the length increases from 5 mm to 10 mm. In addition, the resonance of 1350 MHz band shifted to a lower frequency. As the position S_{LP} moves further away from the feed point, overall higher return loss was observed particularly for the frequency range of 3300-3800MHz.
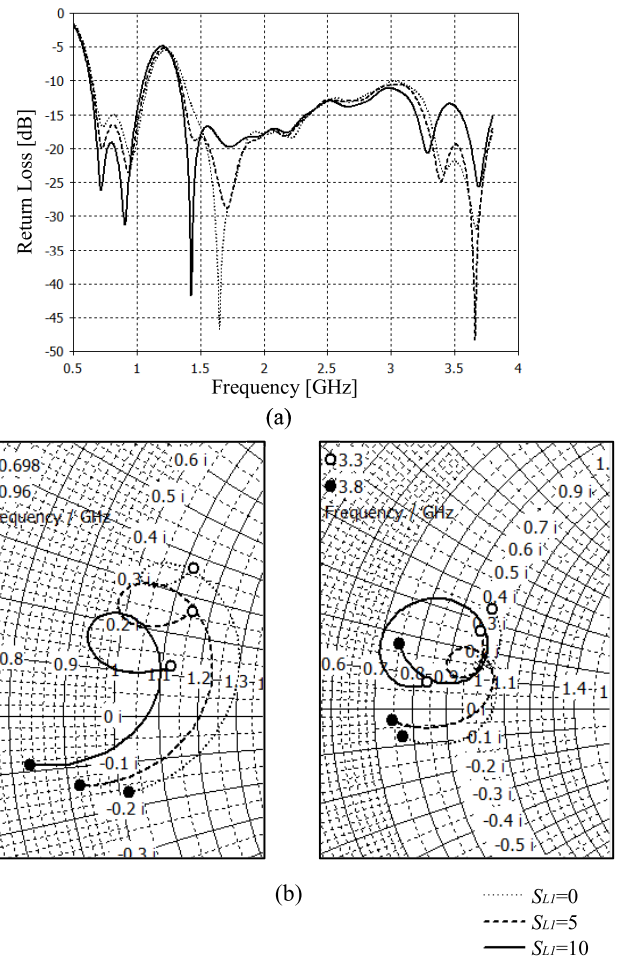

(a)

(b)

$\cdots\cdots$ S_{LI}=0
- - - - S_{LI}=5
——— S_{LI}=10

FIGURE 10. (a) Return loss and (b) impedance locus in zoom-in smith chart of the antenna by varying the slot length at the ground plane S_{L1}.
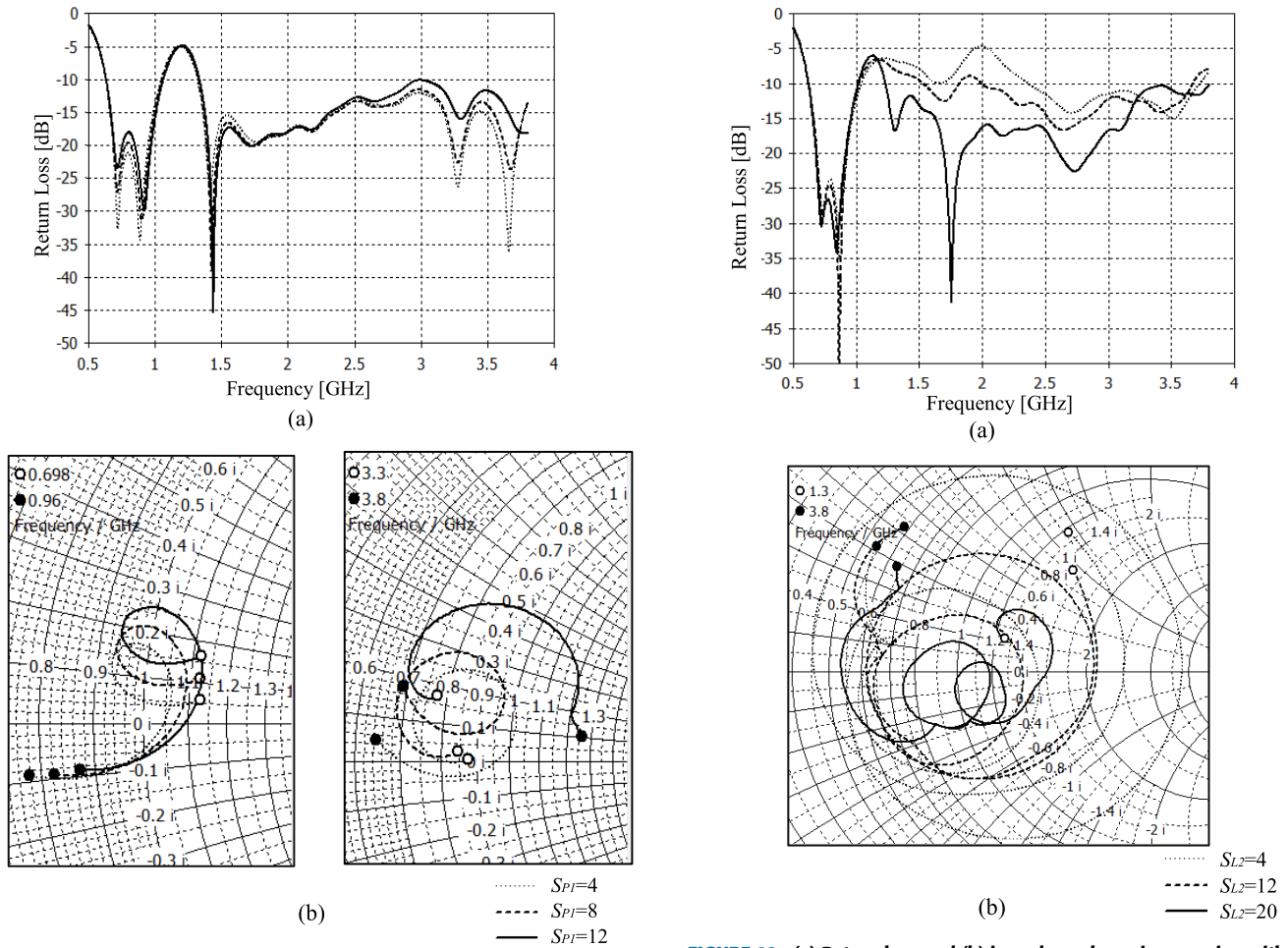
K. J. Ng *et al.*: Azimuth Null-Reduced Radiation Pattern, Ultralow Profile, Dual-Wideband and Low PIM Ceiling Mount Antenna

IEEE *Access*

FIGURE 11. (a) Return loss and (b) impedance locus in zoom-in smith chart of the antenna by varying slot position, *SP1*.
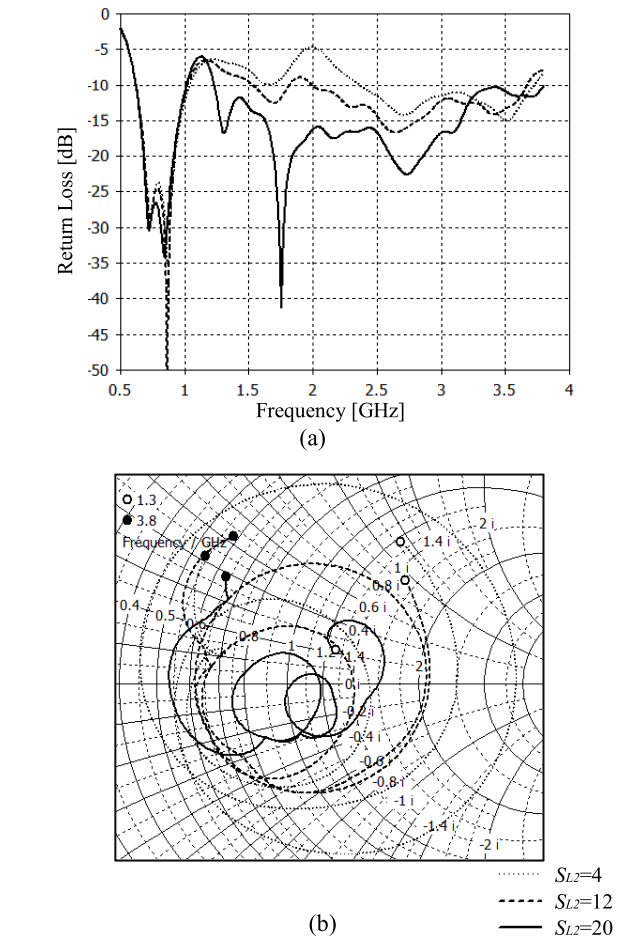

FIGURE 12. (a) Return loss and (b) impedance locus in zoom-in smith chart of the antenna by varying the slot length S_{L2} at radiating element.

Fig. 12 and Fig. 13 show parametric studies on the effect of slot lengths S_{L2} and S_{L3} within the monopole radiator on return loss and impedance locus. Results show that the length of slot S_{L2} has a great impact on the return loss of high-frequency band (1350-3800 MHz) where the optimum length was S_{L2}=20mm. Fig. 12 (b) shows that the impedance locus shrinks as S_{L2} increases. Slot length S_{L3} is generally a less sensitive parameter but it is important for optimization of the 1350-1550 MHz frequency range. Therefore, S_{L3} complements S_{L2} to optimize 1350-1550 MHz frequency band.

Fig. 14 and Fig. 15 show parametric studies on the effect of the gap between the right arm and the feeding edge of the ground plane, Gap_1 and the gap between the left arm and the feeding edge of the ground plane, Gap_2 on the return loss and impedance locus. All other parameters are kept constant. From Fig. 14, we noted that the return loss for frequency beyond 1700 MHz improves when Gap_1 reduces. As shown in Fig. 15, Gap_2 has more impact on the frequency range of 698-1500 MHz where the return loss improves with the increase of $Gap2$. Impedance locus shows that wider $Gap2$
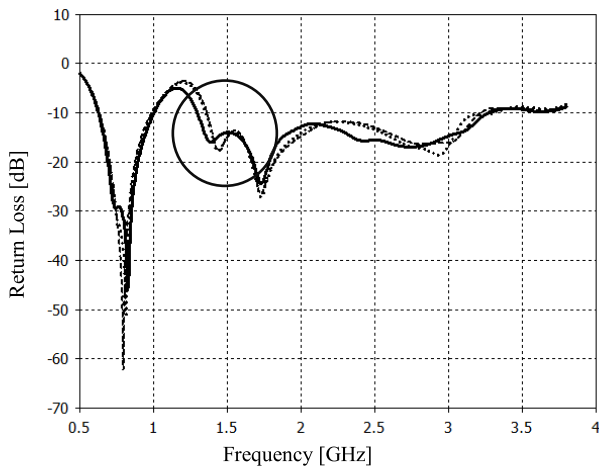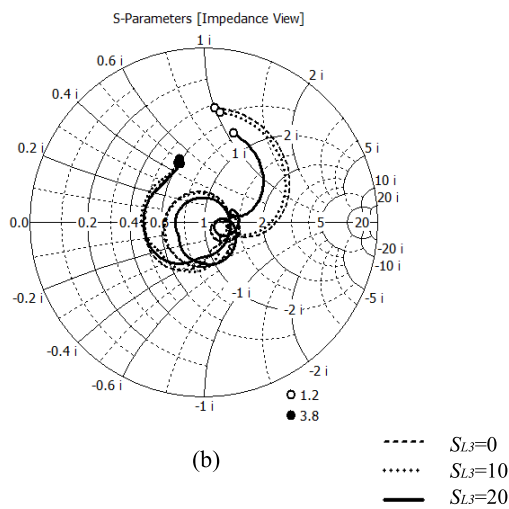
increases the inductance of the antenna in this frequency range that compensates the capacitance. Table 3 summarized the parametric studies on the return loss of the antenna.

E. PIGTAIL CABLE LENGTH EFFECT TO ANTENNA PERFORMANCE

VSWR and radiation pattern are investigated by simulating few pigtail cable lengths, *C_length* of the antenna. Fig. 16 shows pigtail cable length effect on to the simulated VSWR of the antenna. The result shows that the cable effect is more significant at the frequency range of 698-960 MHz and 1400-1500 MHz. However, the antenna still meets the VSWR<2:1 across the desired operating frequency range when the cable length is more than 155mm although there is some unbalanced current flow from the cable. The cable effect at the frequency range of 1.5-3.8 GHz is minimal. The simulated radiation pattern of varying the coaxial cable length, *C_length* of the antenna is shown in Fig. 17. There is no significant variance of radiation pattern except that the null level variance is more significant at a certain angle for the frequency range of 698 MHz-960 MHz.
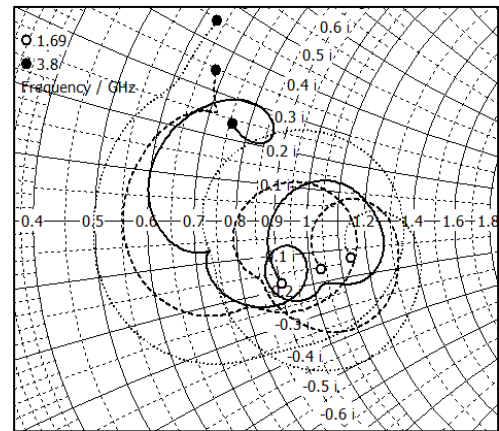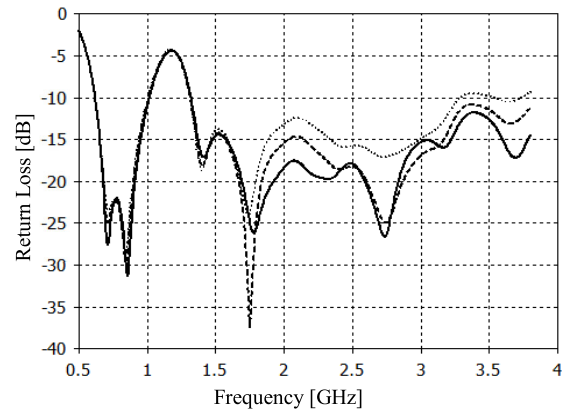
IEEE *Access*

K. J. Ng *et al.*: Azimuth Null-Reduced Radiation Pattern, Ultralow Profile, Dual-Wideband and Low PIM Ceiling Mount Antenna

FIGURE 13. (a) Return loss and (b) impedance locus in zoom-in smith chart of the antenna by varying the slot length S_{L3}. at radiating element.

FIGURE 14. (a) Return loss and (b) impedance locus in zoom-in Smith Chart (1690-3800 MHz) of the antenna by varying Gap_1 between the right arm and the feeding ground plane edge.

F. LOW PIM CONSTRUCTION DESIGN CONSIDERATION

General rules of low PIM construction design focus on avoiding non-linear material or non-linear junction. Non-linear material includes ferromagnetic materials (iron, nickel, cobalt, alloys of magnesium with aluminium, etc.), ferrimagnetic materials (ferrites), dielectric material (alumina 99.7%, etc.). Non-linear junctions may be caused by loose galvanic contact, contaminated surfaces with metal flakes, dirt, dust, moisture or oxidation, rough surface finishing, etc. Based on these important rules, the design put this into design considerations that include dielectric laminates selection, PCB fabrication quality, cable assembly, housing design and antenna assembly process.

Low PIM rated laminate AD300C is selected for the proposed design. Although both substrate material and types of copper foil contribute to PIM performance, the smoothness of the copper foil has the greatest influence on PIM. Therefore, when a laminate is chosen, the smoother foil needs to be specified e.g. reverse treated copper electro-deposited (ED) foil. Effects of foil on PIM performance were investigated in [15].

The substrate material parameters including the dissipation factor, moisture absorption, etc. are factors to be considered too. Lossy material and higher moisture absorption for similar circuit may have higher PIM level. When a softer material like Teflon based substrate is chosen, we noted that high PIM level and inconsistency likely to occur at solder joint between cable assembly and the PCB. The reason was that any movement or pulling will likely to stress the solder joint that may cause microcracking of the solder joint and delamination of the copper foil. By adding proper ribs or plastic material around the solder joint to support, it would reduce the cable movement and stress of solder joint which subsequently minimizes additional PIM generation and inconsistency. This is proven by conducting a pull test on the antenna cable where the PIM is measured before and after the pull test. The PCB copper trace finishing selection may also affect PIM performance. Material such as nickel used in electroless-nickel-immersion-gold (ENIG) plating finishing produces poor PIM performance. Immersion tin is more PIM friendly compared to bare copper and can be used for solder pad that facilitates soldering. The copper layer was also treated with solder mask

K. J. Ng *et al.*: Azimuth Null-Reduced Radiation Pattern, Ultralow Profile, Dual-Wideband and Low PIM Ceiling Mount Antenna

IEEE *Access*

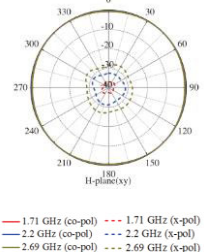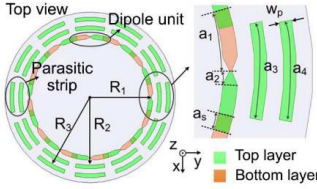**TABLE 3.** Summary of the comparison of the proposed antenna and other works.
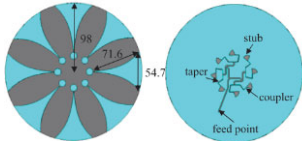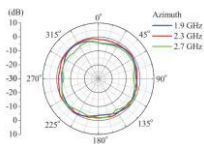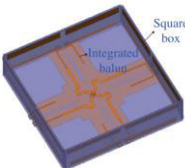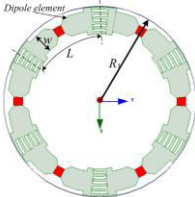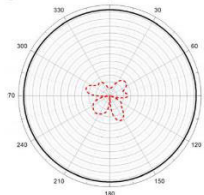
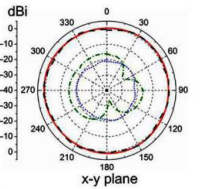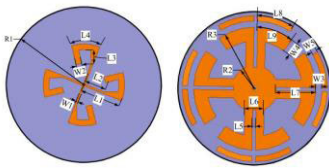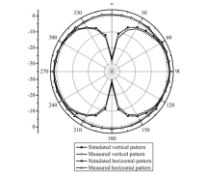| Design	Structure Description	Frequency range (Bandwidth/ Band ratio)	Size	Radiation Pattern when placed horizontally	Other Remarks
[6]	A circular array of eight tapered slots antenna	1.9-2.7 GHz (34.78%/ 1.42:1)	196 mm (Dia.) × 0.8128 mm	Omnidirectional	• Good Omnidirectionality • Single Band and the bandwidth insufficient to cover whole LTE Band • The size will be considered large when considering the frequency of 698 MHz.
[7]	Four wideband dipoles conducted as a loop antenna with parasitic strips	1.64-3.12 GHz (62.1%/ 1.90)	66 mm × 66 mm × 16 mm	Omnidirectional	• Better Omnidirectionality than [6] • Bandwidth better than [6] • Single Band and the bandwidth insufficient to cover whole LTE Band • The size will be considered large when considering the frequency of 698 MHz.
[8]	Six tightly coupled dipole array	4.7-8 GHz (51.96%/ 1.70)	42 mm (Dia.) × 1mm	Omnidirectional 4.8 GHz	• Good Omnidirectionality • Feeding structure has not been investigated and the result is the simulated result. • The size will be considered large when considering the frequency of 698 MHz.
[9]	Twelve printed and tightly coupled arc dipole array with rows of parasitic arc strips and directors	1.7-3.54 GHz (70.2 % / 2.08)	150 mm (Dia.) × 1mm	Omnidirectional 3.2 GHz	• Better Omnidirectionality than [5]&[6] • Bandwidth better than [5] & [6] • Single Band and the bandwidth insufficient to cover whole LTE Band • The size will be considered large when considering the frequency of 698 MHz.
[10]	Four arc printed dipole array with four pairs of parasitic strips	2.23-4.11 GHz (59.3%/ 1.84)	80 mm (Dia.) × 1.6 mm	Omnidirectional 3.5 GHz	• Good Omnidirectionality • Bandwidth better than [5] & [8] • Single Band and the bandwidth insufficient to cover whole LTE Band • The size will be considered large when considering the frequency of 698 MHz.

IEEE *Access*

K. J. Ng *et al.*: Azimuth Null-Reduced Radiation Pattern, Ultralow Profile, Dual-Wideband and Low PIM Ceiling Mount Antenna

TABLE 3. *(Continued.)* **Summary of the comparison of the proposed antenna and other works.**
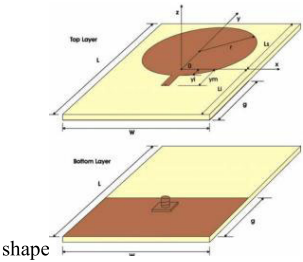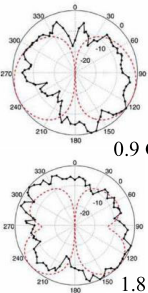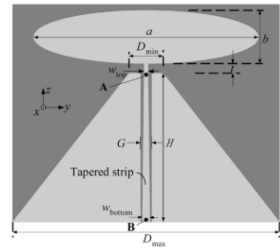
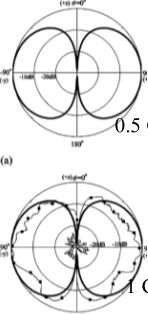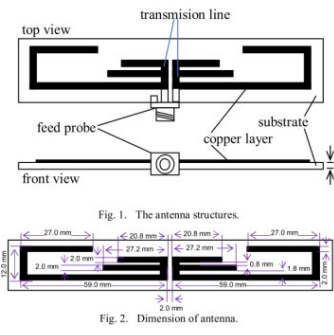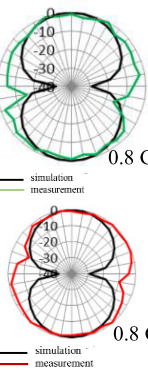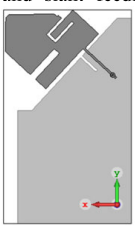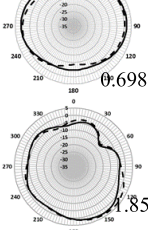|					
[11]	The asymmetrical dipole of circular shape	0.7986-17.4663 GHz (182.5%/ 14.9:1)	90 mm × 135 mm× 1.575 mm	Elevation planar monopole liked 0.9 GHz 1.8 GHz	• Bandwidth is sufficient to cover the full LTE band • However, the design investigation does not include any azimuth null reduction radiation pattern. • The radiation pattern is not omnidirectional in horizontal and the simulated result shows deep null. The measured radiation pattern does not conform very well with simulated. • The feed is perpendicular to the antenna plane, but the cable effect is not been investigated.
[12]	Elliptical monopole on trapezoid ground plane	0.4-9.51 GHz (184%/ 21.6:1)	140mm × 107.3mm× 1.524 mm	Elevation planar dipole liked 0.5 GHz 1 GHz	• Bandwidth is sufficient to cover the full LTE band • However, the design investigation does not include any azimuth null reduction radiation pattern. • The radiation pattern is not omnidirectional in horizontal. Both measured and simulated radiation pattern shows deep null in the horizontal plane • The feed is parallel to the antenna plane.
[13]	Multiple folded radiating elements with multiband	800 MHz, 1700 MHz and 2300 MHz (16.5%,21.3% and 16.7 %)	120mm × 16mm × 1.6 mm	Elevation planar dipole liked 0.8 GHz simulation measurement 0.8 GHz simulation measurement	• Bandwidth is insufficient to cover the full LTE band • However, the design investigation does not include any azimuth null reduction radiation pattern. • The radiation pattern is not omnidirectional in horizontal. Measured radiation pattern shows discrepancies compared to simulated. • Simulated result shows deep null in design. • The feed is parallel to the antenna plane.
Proposed	Offset Monopole offset feeding point and slant feeding edge ground plane	0.698 GHz - 0.96 GHz and 1.35-3.80 GHz (31.6% and 95.1%)	90 mm × 151 mm × 0.76 mm	0.698 GHz 1.85 GHz	• Bandwidth covers the full LTE band • Radiation pattern with reduced null at azimuth plane when placed horizontally. • Offset Monopole • Offset feeding point • Slanting feeding edge • Multiple arms.

K. J. Ng et al.: Azimuth Null-Reduced Radiation Pattern, Ultralow Profile, Dual-Wideband and Low PIM Ceiling Mount Antenna

IEEE Access

TABLE 3. *(Continued.)* **Summary of the comparison of the proposed antenna and other works.**

- A perpendicular feed with pigtail cable
- Low PIM construction that considers material, design and process for consistent performance.
- Real practical antenna in the field.

Note:

1. LTE Band includes 0.698-3.8 GHz will need the bandwidth of 137.92 % or band ratio of 5.44 in a single band.

2. Most of the reference is not considering the cable effect. The proposed design considered in the field application includes the pigtail cable in simulation and prototype which may provide better accuracy of the radiation pattern.
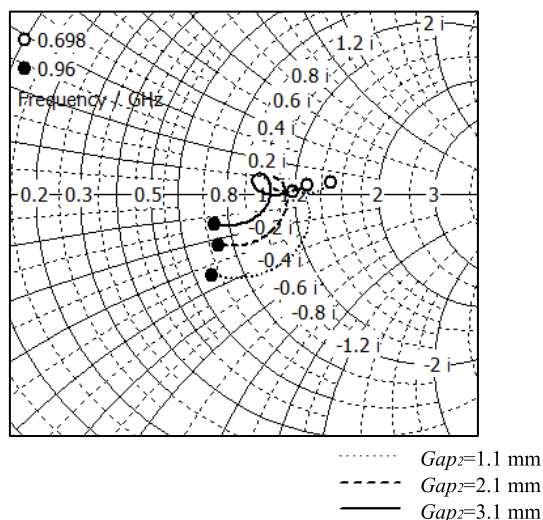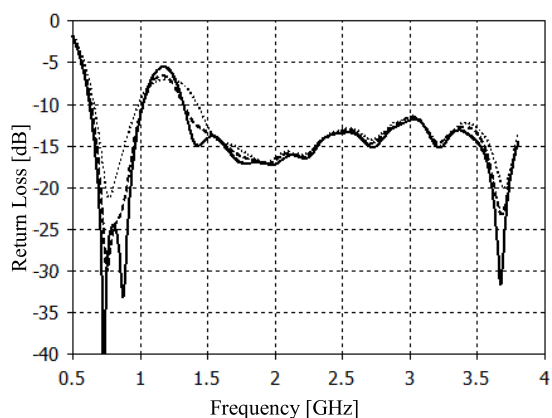

FIGURE 16. Simulated VSWR of the antenna by varying the coaxial cable length, *C_length* of the antenna for the parametric study.

FIGURE 15. (a) Return loss and (b) impedance locus in zoom-in Smith Chart (698-960MHz) of the antenna by varying *Gap₂* between the left arm and the feeding ground plane edge.

General guides on PCB selection and other built process are described in [16], [17]. Another important feature of low PIM PCB design is that the solder pad dimension needs to be optimized with the right pull back dimension of the copper trace to facilitate a consistent and ease of soldering process, thus resulting in good wetting quality.

The cable assembly for the antenna needs to be built with care. The material used for the construction of semi-flexible RG402 and Type-N connector must be low PIM rated. To prepare the cable, it must have a clean-cut during the stripping process. Then the cable is terminated with N connector by using either resistance soldering or induction soldering depending on the connector design and plating composition. Cable crimping method must be avoided as it has a high risk of PIM generation. The PIM performance of the cable assembly must be verified to be below -160 dBc (with carrier input powers of 2×20 dBm) before soldered to the PCB.

The top housing was designed such that it can be assembled to the plastic baseplate directly without any metal fastener, with the PCB sandwiched in between them. It utilized the snap feature at the edge of both the plastic parts and plastic heat-staking to hold all the parts together easily. This eliminates any potential PIM source due to the metal fastener. The design of the antenna was very simple where the most

to protect the entire trace from contamination and exposure to air or humid. We noted that not all PCB fabricators are capable to produce high-quality low PIM PCB antenna. Fabricator needs to ensure that the etched copper trace is of good quality and uniform. In addition, all the processes need to include careful cleaning to eliminate the possibility of contamination.
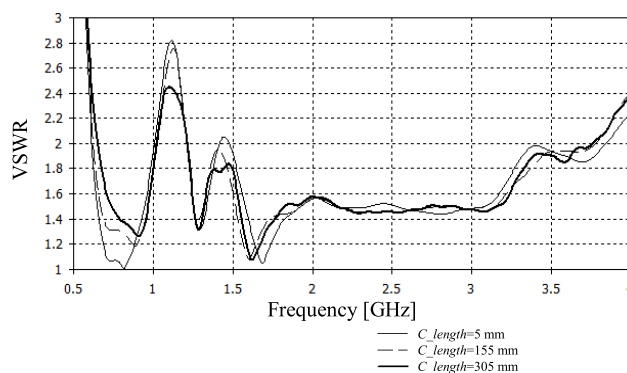
IEEE *Access*

K. J. Ng *et al.*: Azimuth Null-Reduced Radiation Pattern, Ultralow Profile, Dual-Wideband and Low PIM Ceiling Mount Antenna

with suitable soldering station with the optimum power rating, temperature, solder tip and right skill. After the soldering process, the solder joint need to be cleaned with solvent clean away any residue metallic particles/flakes, flux and burned mark. Based on observation, poor wetting resulting from improper soldering process can cause the rise of PIM level for all the bands. We noted that poor wetting at the edge of solder joint and contamination may result in the rise or inconsistency of PIM at higher frequency range. Another scenario that may cause the poor PIM level is when solder joint degrades due to multiple times of re-flows.

III. FABRICATION AND MEASUREMENT

Fig. 18 shows the photo of the prototype with translucent polycarbonate thermoplastic housing enclosing the PCB antenna and the bare PCB in both top and bottom view. Typical in-house PCB rapid prototyping facility using mechanical etching is not able to meet the quality needs for best PIM performance and the good alignment of *Gap1* and *Gap2*. Therefore, production-quality PCB has been made by PCB fabricator to verify the performance of the antenna.
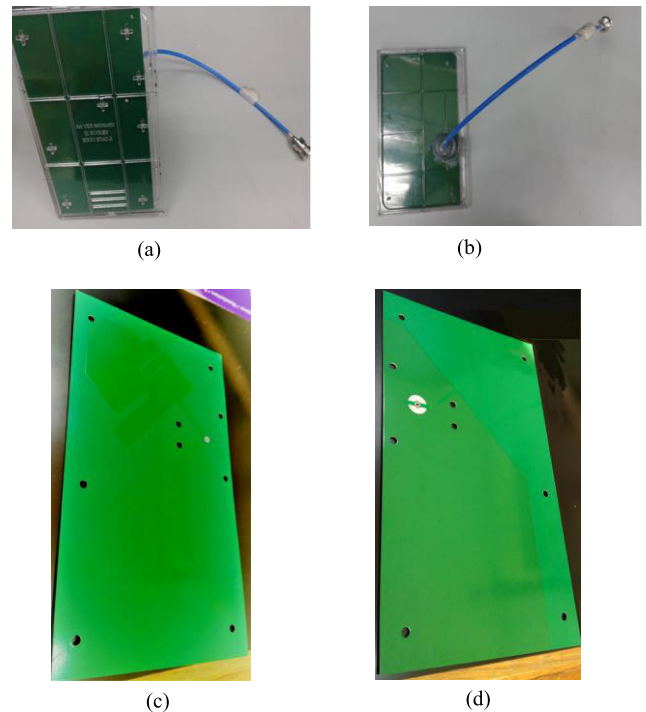
FIGURE 18. Photo of the prototype where the plastic radome is machined with Polycarbonate in translucent. (a) Top view, (b) Back view, (c) PCB top view and (d) PCB bottom view.

Fig. 19 shows the VSWR measurement setup using Copper Mountain Planar 804/1 Vector Network Analyzer (VNA) and the antenna is placed on a test fixture inside the 4'×4'×4' mini anechoic chamber with the pyramidal absorber. Fig. 20 shows the measured and simulated VSWR of the antenna. The result shows that the measurement correlates well with the simulation. However, the measured result shows some ripples due to the long cable and mismatch of the
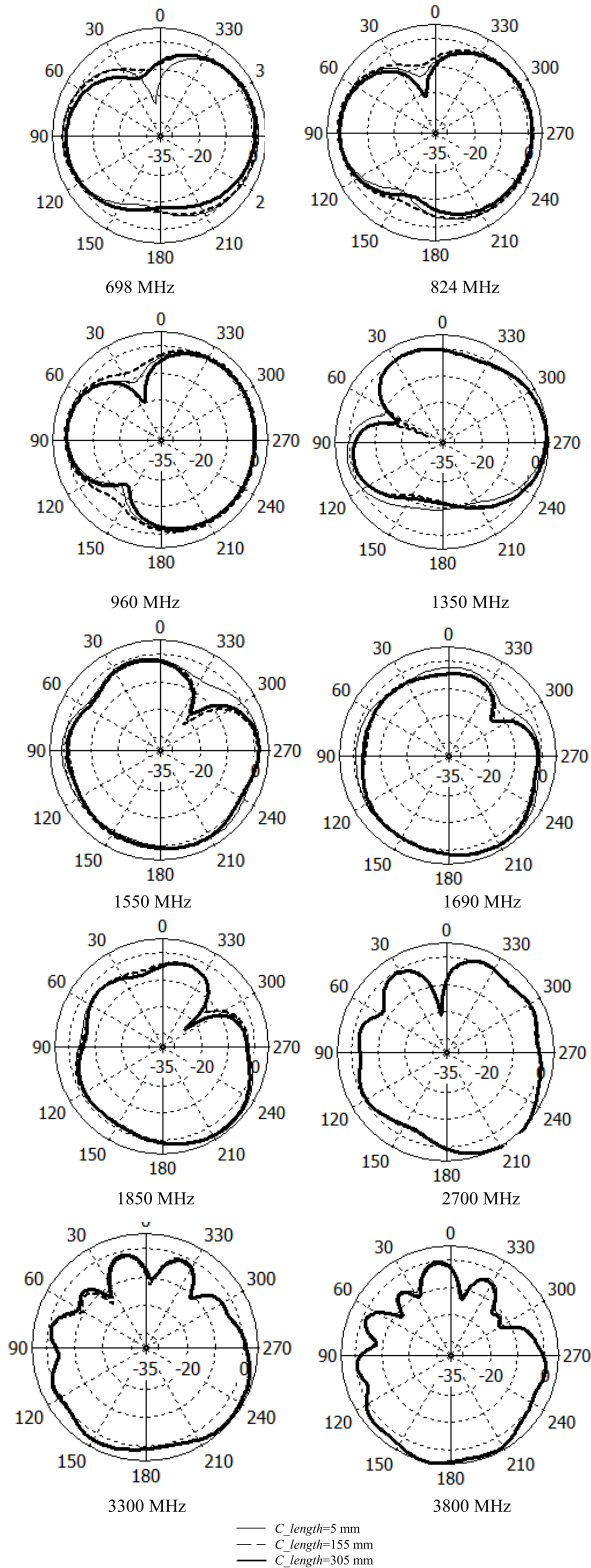
FIGURE 17. The simulated radiation pattern of the antenna by varying the coaxial cable length, **C_length** of the antenna for the parametric study.

important galvanic contact is the solder joint between the cable and the PCB. Although the solder pad dimension has been optimized, the soldering process needs to be performed

K. J. Ng *et al.*: Azimuth Null-Reduced Radiation Pattern, Ultralow Profile, Dual-Wideband and Low PIM Ceiling Mount Antenna
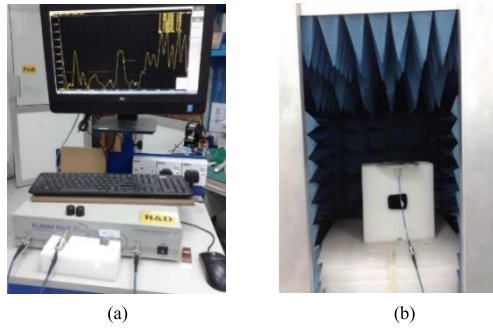
IEEE *Access*

FIGURE 19. (a) The photo of VNA Planar 804/1 and (b) the antenna placed on a test fixture inside the 4′ × 4′ × 4′ chamber.
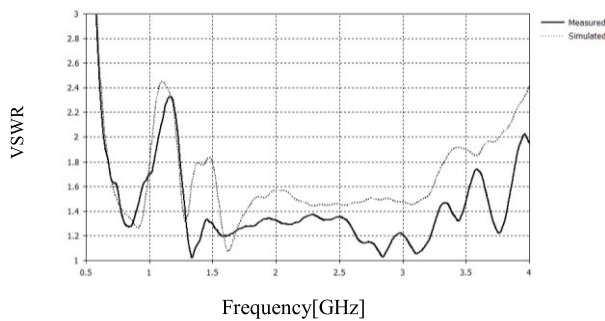

FIGURE 20. The simulated and measured VSWR of the antenna.

connector which was not included in the simulation model. The antenna meets VSWR <2:1 for the frequency ranges of 698-960MHz and 1350-3800MHz.

The radiation pattern of the antenna was measured by using Satimo SG24 near-field 3D measurement system as shown in Fig. 21. The measurement system consists of 23 probes arranged in a stargate form that measure the near-field radiation of the antenna and will then transformed into far-field result. Figure 22 shows the simulated and measured radiation patterns at various frequency points in the horizontal plane (Azimuth plane). The plot shows the simulated result correlates well with the measured result. For the sake of brevity, the elevation plane is not presented in this paper. The measured radiation pattern for the low-frequency band
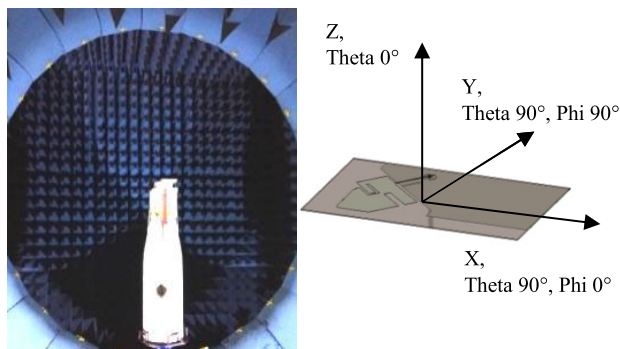

698 MHz   824 MHz

960 MHz   1350 MHz

1550 MHz   1690 MHz

1850 MHz   2700 MHz

3300 MHz   3800 MHz

- - - - Simulated
——— Measured

FIGURE 22. The simulated and measured radiation pattern of the proposed antenna design at Azimuth Plane.

of (698-960 MHz) has a better null condition compared to the simulated result. This is a significantly improved radiation pattern compared to the conventional dipole antenna.

For the mid-frequency range of 1350-1550 MHz, the measured radiation pattern shows slightly deeper null and lower gain at certain angles compared to the simulated result. Fig. 23 (a) shows both measured and simulated peak gain of the antenna across the operating frequency range of interest.

FIGURE 21. Measurement setup and coordinate system for the radiation pattern measurement of the antenna.
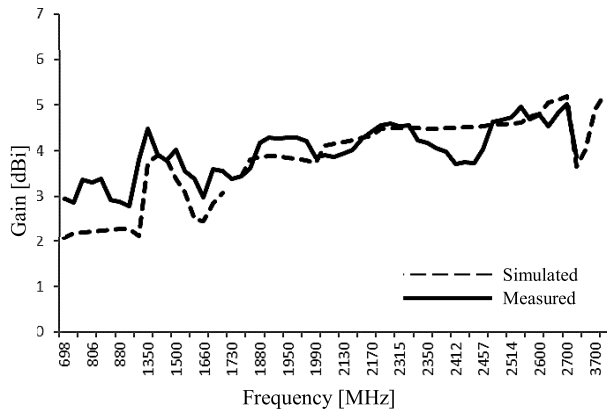
(a)
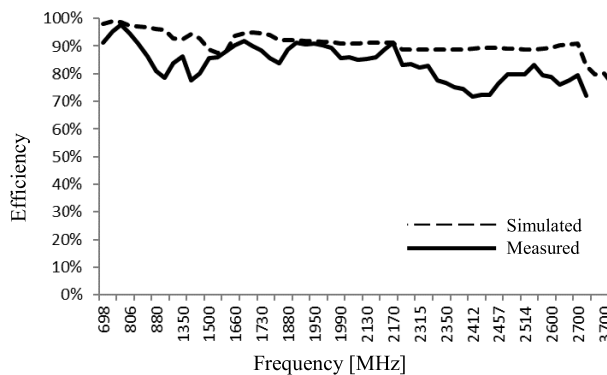
(b)

FIGURE 23. Comparison of the measured and simulated (a) peak gain and (b) efficiency of the antenna across the operating frequency.

The simulated gain correlates well with the measurement result. Fig. 23 (b) depicts the measured and simulated total efficiency of the antenna. The measured total efficiency is typically lower than the simulated result but the average efficiency of 84% across the frequency range of interest.

As the antenna is designed with low PIM, the PIM measurement was performed with the measurement setup shown in Fig. 24. The third order PIM level is measured with two tones of 20W frequency carrier excited into the antenna that placed in a 10' ×10' ×10' anechoic PIM chamber. The measurement was performed with commercial PIM analyzers, i.e. Kaelus iQA-700 HC and iQA-1920C that measure PIM for 700 MHz band and 1920 MHz band respectively. These two frequency bands are used to represent the PIM level of the low-frequency band and high-frequency band respectively. PIM measurement is based on the reverse measurement setup. The frequency sweep mode is used for the measurements. The measurement is set up for 7 s seconds of frequency sweep to ensure a consistent result achieved over the period. The inconsistent result may occur if soldering of the cable to the PCB was not performed well or the cable assembly was not properly assembled. For the 700 MHz band, the transmitted frequency carriers sweep between 728 MHz to 757 MHz where
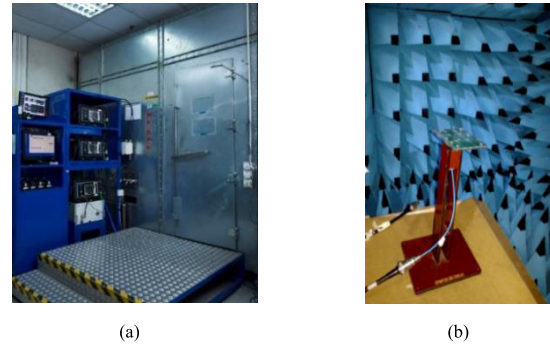

(a)   (b)

FIGURE 24. (a) The PIM tester and chamber and (b) the antenna placed on a fixture inside the PIM anechoic chamber.

the third-order PIM measurement was taken for the frequency range from 776 MHz to 786 MHz. For 1920 MHz band, the transmitted frequency carriers sweep between 1930 MHz to 1990 MHz where the third-order PIM measurement was taken in the frequency range from 1870MHz to 1910 MHz. The peak of the third-order PIM level must be below the common specification for DAS applications of −150 dBc. The prototype measurement results in Fig. 25. shows that it has the maximum PIM level of −158.9 dBc and -153.5 dBc respectively for 700 MHz band and 1920 MHz band.
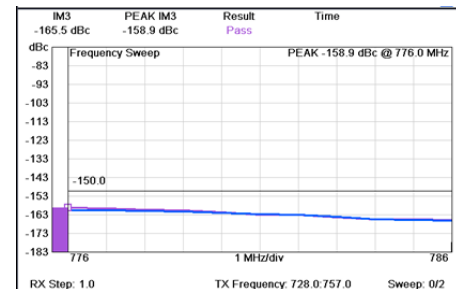
(a)
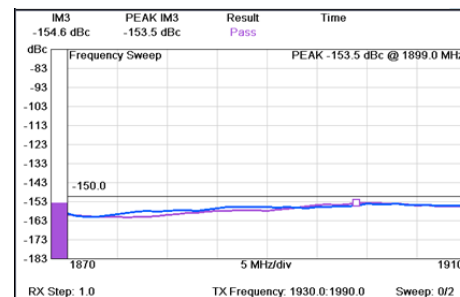
(b)

FIGURE 25. The PIM measurement result at (a) 700 MHz band and (b) 1920 MHz band.

Table 3 shows the summary comparison of the proposed antenna and other designs. The discussed works [6]–[10] are arrays that achieved good omnidirectionality in horizontal polarization but may have a large size when considering the frequency of 698 MHz. Dipoles in [11]–[13] represent different types of dipole may have deep null at azimuth plane

K. J. Ng *et al.*: Azimuth Null-Reduced Radiation Pattern, Ultralow Profile, Dual-Wideband and Low PIM Ceiling Mount Antenna

IEEE*Access*

when placed horizontally as expected. None of this work considers pigtail application and the design have not considered the cable effect that may have a higher discrepancy of the radiation pattern. As noted, these antennas do not include any balun design. The proposed design visually seem to be simple and common but the detail characterization shows improved radiation pattern from deep null of the elevation plane dipole radiation pattern placed in the horizontal plane. The design has better VSWR (not merely <2:1) to enable the performance maintained with <2:1 when there is any detuning effect to the antenna. Besides that, the proposed antenna has considered the low PIM construction in design to have consistent performance in mass production.

IV. CEILING TILE AND FRAME EFFECT

As the proposed was designed based on the asymmetrical dipole, the application will be limited to the mineral and fiber-filled ceiling material. Any metal-backed ceiling or metal ceiling will detune the antenna significantly. In order to verify the effect of this mineral and fiber filed material, the antenna was placed on top of 600mm × 600mm × 15mm standard acoustic tile for measurement. As limited by the size of the antenna under test in the available chamber, 600mm × 600mm × 15mm standard acoustic tile is chosen for the measurement instead of the common 600mm × 1200mm × 15mm ceiling tiles. In addition to the ceiling tiles effect, the frame of three sides of the edge that represents half of the 600mm × 1200mm × 15mm ceiling tile installation was measured as well. Fig. 26 shows the comparison of measured VSWR of the antenna on (a) free space, (b) acoustic ceiling tile and (c) acoustic ceiling tile with frame. The result depicts minimal effect on the VSWR. However, the result may be different from those ceiling tiles with different density, thickness, and hardness. Therefore, the impact can be still minimal as the proposed design elevated the PCB that does not have direct dielectric-loaded due to the ceiling tile. The radiation pattern was also measured on these configurations and shown in Fig. 27. It is observed that the material has minimal impact. However, we can observe more ripple to the radiation pattern for the frequency range from 824 MHz to 1850 MHz.when the antenna measured with acoustic ceiling tiles with frame
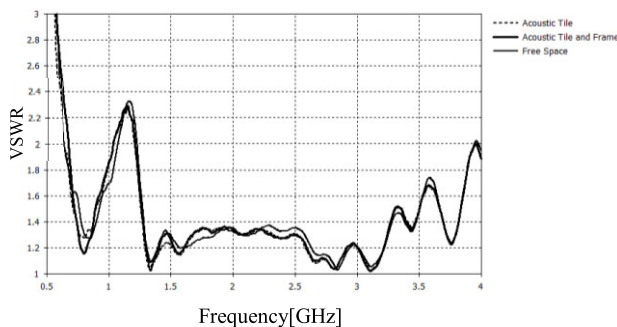
FIGURE 26. Comparison of VSWR when antenna mounted onto ceiling tiles condition and ceiling tiles with frame.
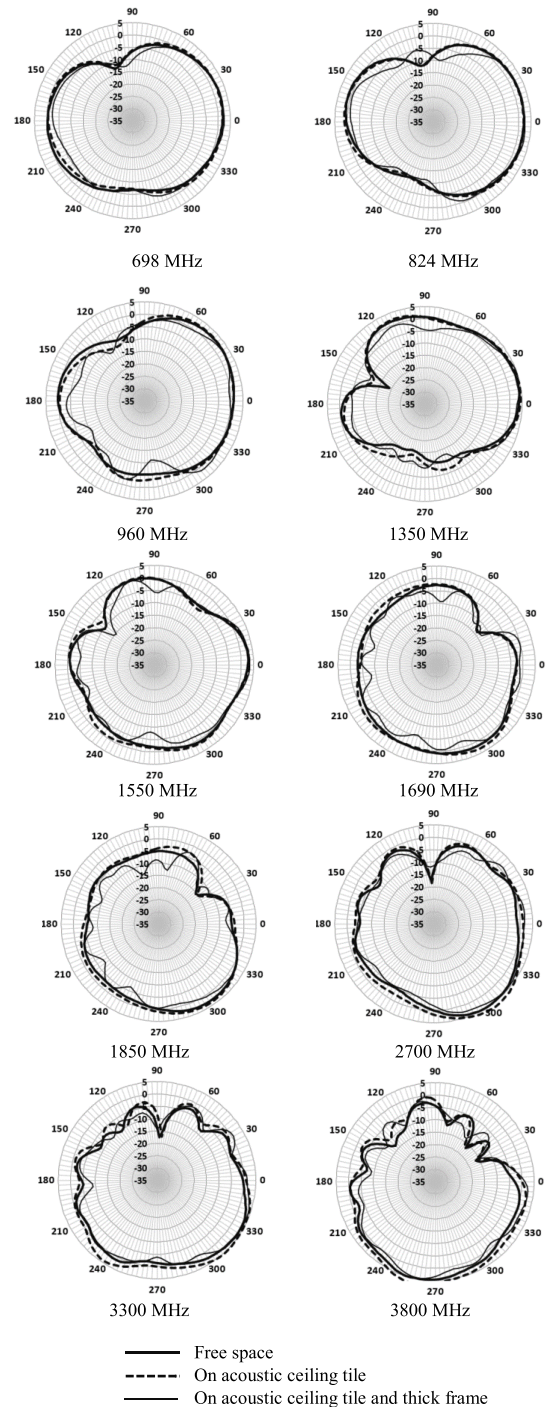
FIGURE 27. Comparison of radiation pattern when antenna mounted onto ceiling tiles condition and ceiling tiles with frame.

V. CONCLUSION

Investigation of dipole and monopole of type-I to type-IV was presented. Type-IV which uses simple offset fed rectangular monopole and offset feeding location at the ground plane gives reduced null (oriented horizontally) at most of the frequencies compared to other dipoles/monopoles types. To further improve the design, a novel design based on asymmetrical dipole that has offset fed monopole radiating

IEEE Access

K. J. Ng *et al.*: Azimuth Null-Reduced Radiation Pattern, Ultralow Profile, Dual-Wideband and Low PIM Ceiling Mount Antenna

element with offset feeding location on an inclined feeding edge of a ground plane was presented. These give more design freedoms that offer a good compromise between the VSWR and the reduced null radiation pattern at the azimuth plane. To validate the performance, a prototype was fabricated with production-ready quality to ensure the best achievable PIM performance. The comparison between the simulated and measured results for VSWR and radiation pattern was presented. The simulation results correlate well to the measurement results. The proposed design shows dual-wideband characteristic with achievable bandwidth of 31.6% with respect to the center frequency of 829MHz and 95.1% with respect to the center frequency of 2575MHz covering most of the LTE range. The radiation pattern of the proposed design offers reduced null in the Azimuth plane across the frequency range of interest compared to the conventional dipole design. This perspective is considered as a new class of ceiling type antenna that partially compensates the weakness of the radiation pattern of a horizontally oriented dipole to achieve ultralow profile feature flushing to the ceiling. In addition, the third-order PIM level with carrier inputs of $2 \times .20$W was measured and meet the typical DAS PIM requirement of $<$-150 dBc with the levels of -158.9 dBc and -153.5 dBc achieved for 700 MHz band and 1920 MHz band respectively. The ceiling material and frame effect on the VSWR and radiation pattern were presented too.

REFERENCES

[1] D. W. Aten and R. L. Haupt, "A wideband, low profile, shorted top hat monocone antenna," *IEEE Trans. Antennas Propag.*, vol. 60, no. 10, pp. 4485–4491, Oct. 2012.

[2] L. Zhou, Y. Jiao, Y. Qi, Z. Weng, and L. Lu, "Wideband ceiling-mount omnidirectional antenna for indoor distributed antenna systems," *IEEE Antennas Wireless Propag. Lett.*, vol. 13, pp. 836–839, 2014.

[3] L. Januszkiewicz and S. Hausman, "Combined spiral-discone broadband antenna for indoor applications," in *Proc. IEEE 15th Int. Symp. Pers., Indoor Mobile Radio Commun.*, Sep. 2004, vol. 1, no. 1, pp. 422–426.

[4] K. He, S.-X. Gong, and D. Guo, "Broadband omnidirectional distributed antenna for indoor wireless communication systems," *Electron. Lett.*, vol. 52, no. 16, pp. 1361–1362, Aug. 2016.

[5] H. Nakano, M. Takeuchi, and J. Yamauchi, "Modified wideband BOR-SPR antenna," in *Proc. IEEE-APS Top. Conf. Antennas Propag. Wireless Commun. (APWC)*, Sep. 2015, pp. 55–57.

[6] Y.-F. Yu, Q.-F. Dai, and L.-L. Chen, "Wideband horizontally polarized omnidirectional antenna," in *Proc. Prog. Electromagn. Res. Symp. (PIERS)*, 2016, pp. 102–104.

[7] L. H. Ye, Z. J. Zhang, W. Duan, and X. Y. Zhang, "Wideband horizontally polarized omnidirectional antenna with small size," in *Proc. Int. Symp. Antennas Propag. (ISAP)*, Oct. 2018, pp. 1–2.

[8] Y. Liu, H. Liu, and S. Gong, "A wideband horizontally polarized omnidirectional antenna using tightly coupled array mechanism," in *Proc. Int. Work. Antenna Technol. Small Antennas, Innov. Struct., Appl. (iWAT)*, Mar. 2017, pp. 135–136.

[9] Z. D. Wang, Y. Z. Yin, X. Yang, and J. J. Wu, "Design of a wideband horizontally polarized omnidirectional antenna with mutual coupling method," *IEEE Trans. Antennas Propag.*, vol. 63, no. 7, pp. 3311–3316, Jul. 2015.

[10] S. Chen, Y. Sun, and D. Zhou, "A wideband omnidirectional horizontally polarized antenna for wireless applications," in *Proc. 9th IEEE Int. Conf. Microw. Millim. Wave Technol. (ICMMT)*, Jun. 2016, vol. 2, pp. 713–715.

[11] S. Barbarino and F. Consoli, "Study on super-wideband planar asymmetrical dipole antennas of circular shape," *IEEE Trans. Antennas Propag.*, vol. 58, no. 12, pp. 4074–4078, Dec. 2010.

[12] S.-S. Zhong, X.-L. Liang, and W. Wang, "Compact elliptical monopole antenna with impedance bandwidth in excess of 21:1," *IEEE Trans. Antennas Propag.*, vol. 55, no. 11, pp. 3082–3085, Nov. 2007.

[13] Iswandi, A. K. D. Jaya, and E. S. Rahayu, "Design of triple band printed dipole antenna for indoor small cell base station in LTE systems," in *Proc. 2nd Int. Conf. Inf. Technol., Inf. Syst. Electr. Eng.*, Nov. 2017, pp. 207–210.

[14] J. Sanford, "Passive intermodulation considerations in antenna design," in *Proc. IEEE Antennas Propag. Soc. Int. Symp.*, Jun./Jul. 1993, pp. 1651–1654.

[15] A. G. Schuchinsky, J. Francey, and V. F. Fusco, "Distributed sources of passive intermodulation on printed lines," in *Proc. IEEE Antennas Propag. Soc. Int. Symp.*, vol. 4B, Jul. 2005, pp. 447–450.

[16] J. Coonrod, "Choosing circuit materials for low-PIM PCB antennas," Microw. RF, Tech. Marketing Manager Rogers Corp., Adv. Connectivity Solutions, Chandler, AZ, USA, Tech. Rep., Nov. 2017. [Online]. Available: https://www.mwrf.com/components/choosing-circuit-materials-low-pim-pcb-antennas

[17] B. Collins, "Base station antennas for mobile radio systems," in *Antennas for Base Stations in Wireless Communications*, Z. N. Chen and K.-M. Luk, Eds. New York, NY, USA: McGraw-Hill, 2009, pp. 31–94.

[18] *CFSA Series—Public Safety | Laird Connectivity*. Accessed: Dec. 11, 2018. [Online]. Available: https://connectivity.lairdtech.com/rf-antennas/land-mobile-radio-antennas/public-safety-das-antennas/cfsa-series-public-safety#documentation

[19] K. J. Ng, C. C. Su, and C. Y. Hang, "Low profile omnidirectional antennas," U.S. Patent 10 205 241 B2, Feb. 12, 2019.

KOK JIUNN NG was born in Teluk Intan, Perak, Malaysia, in 1977. He received the B.Eng. and M.S. degrees in electrical, electronic and system engineering from the National University of Malaysia, in 2000 and 2004, respectively. He is currently pursuing the Ph.D. degree with the National University of Malaysia.

From 2004 to 2006, he was a Research Engineer with the Anscom Sdn. Bhd. He was an RF Engineer with Laird Technology (M) Sdn. Bhd. and a Senior RF Engineer with Amphenol Antenna Solution (M) Sdn. Bhd., from 2006 to 2007. Since 2008, he has been with Laird Technologies (M) Sdn. Bhd. and he is currently a Snr. Staff Engineer with the Advance Technology Group, Antenna Division. He holds more than ten patents. His research interests include embedded antenna, portable land mobile antenna, MIMO antenna, DAS antenna, array antenna, and PIM.

K. J. Ng *et al.*: Azimuth Null-Reduced Radiation Pattern, Ultralow Profile, Dual-Wideband and Low PIM Ceiling Mount Antenna

IEEE*Access*

MOHAMMAD TARIQUL ISLAM is currently a Professor with the Department of Electrical, Electronic and Systems Engineering, Universiti Kebangsaan Malaysia (UKM) and a Visiting Professor of the Kyushu Institute of Technology, Japan. He is the author and coauthor of about 450 research journal articles, nearly 175 conference articles, and a few book chapters on various topics related to antennas, microwaves, and electromagnetic radiation analysis with 18 inventory patents filed. Thus far, his publications have been cited 4500 times and his H-index is 34 (Source: Scopus). His Google scholar citation is 6050 and H-index is 38. His research interests include communication antenna design, radio astronomy antennas, satellite antennas, and electromagnetic radiation analysis.

Dr. Islam is also a Chartered Professional Engineer-CEng, a member of IET, U.K., and a member of IEICE, Japan. He was a recipient of more than 40 research grants from the Malaysian Ministry of Science, Technology and Innovation, Ministry of Education, UKM Research Grant, International Research Grants in Japan and Saudi Arabia. He received several International Gold Medal Awards, the Best Invention in Telecommunication Award, a Special Award from Vietnam for his research and innovation, and the Best Researcher Awards from UKM, in 2010 and 2011. He was a recipient of the 2018 IEEE AP/MTT/EMC Excellent Award. He also received the Best Innovation Award, in 2011 and the Best Research Group in ICT Niche from UKM, in 2014. He was a recipient of Publication Award from Malaysian Space Agency, in 2009, 2010, 2013, and 2014, and the Best Paper Presentation Award, in 2012 International Symposium on Antennas and Propagation, (ISAP 2012) at Nagoya, Japan, and, in 2015 at IconSpace. He also serves as a Guest Editor for *Sensors Journal* and an Associate Editor for the IEEE Access and IET Electronics Letter.

ADAM ALEVY received the B.S. degree in electrical engineering from Northeastern University, Boston, MA, USA, in 1987.

From 1987 to 1995, he was an Antenna Design Engineer with D&M Chu Technology, Littleton, MA, USA, (formerly Chu Associates), where he worked on various antennas for Radar, Communication, and Satcom Systems, from 3 MHz to 20 GHz. From 1994 to 1997, he was employed as an Antenna Engineer with the Atlantic Microwave Division, Cobham PLC, Bolton, MA, USA. At Atlantic Microwave, he designed and managed the development of antenna systems from VHF to 50 GHz for various military applications. Since 1998, he has been with Laird Technologies (Cushcraft Corporation). He is currently the Sr. Director of technology with the Antenna Division, Laird Connectivity. In this role, he manages the team in the development of antennas for commercial Wi-Fi, Telecom, the Internet of Things, and Public Safety systems. He holds three patents in antenna design. He is also an Eta Kappa Nu.

MOHD. FAIS MANSOR (M'09) was born in Selangor, Malaysia, in 1981. He received the B.Eng. (computer and communication) from UKM, in 2005, and the Ph.D. (Antenna and Propagation) from the University of Surrey, U.K., in 2012.

He has been with UKM, since 2005, where he is currently a Senior Lecturer with the Centre of Advanced Electronic and Communication Engineering and the coordinator of UKM International Office, UDE. Since 2008, he has been involved in MIMO antenna design and evaluation with special focus on Satellite MIMO System. He was a Visiting Researcher with the Institute of Digital Signal Processing, University of Duisburg-Essen (UDE), Germany, from August 2017 to July 2018, in MARIE Project supported by the German Research Foundation. His main areas of research interests include MIMO antenna design and evaluation, reconfigurable antennas, and mm-wave antennas and RF circuits.

CHOON CHUNG SU received the B.E. degree in electronic and communications engineering, and the M.Eng.Sc. degree in microwave engineering and antenna designs from Tunku Abdul Rahman University, Kuala Lumpur, Malaysia, in 2010 and 2014, respectively. He is currently serving for Laird Technologies (M) Sdn. Bhd. and as an RF Engineer with the Research and Development Department responsible for the design and development of antenna products.

● ● ●